

**Supplementary information**

---

**Concept, implementations and applications of Fourier ptychography**

---

In the format provided by the authors and unedited

# Supplementary Note for *Nature Physics Review*

## Setting up a Fourier ptychographic microscopy platform

Guoan Zheng<sup>1\*</sup>, Cheng Shen<sup>2</sup>, Shaowei Jiang<sup>1</sup>, Pengming Song<sup>1</sup>, and Changhui Yang<sup>2\*</sup>

<sup>1</sup>Department of Biomedical Engineering, University of Connecticut, USA

<sup>2</sup>Department of Electrical Engineering, California Institute of Technology, USA

\*Email: [guoan.zheng@uconn.edu](mailto:guoan.zheng@uconn.edu), [chyang@caltech.edu](mailto:chyang@caltech.edu)

### 1. Programmable LED array

To set up a Fourier ptychography (FP) experiment, one can use an LED array for angle-varied illumination. The LED element is preferably to be small and bright. Figure S1 shows a 16 by 16 programmable LED array built with small surface mounted device (SMD) LEDs (Adafruit product ID: 3341). The pitch is  $\sim 2.5$  mm and the size of the entire array is less than 4 cm. Some random offsets can also be introduced to the row or column to avoid periodic sampling in the Fourier domain<sup>1</sup>. Similar 8 by 8 LED array is commercially available by Adafruit (product ID: 3444). Since the LED elements are densely packed, they can provide a larger Fourier overlapping ratio for FP. As a result, one can bring the array closer to the specimen to achieve a higher optical flux reaching the specimen. The array can also be placed at the back focal plane of a condenser lens for angle-varied illumination<sup>2,3</sup>, as shown in Fig. S2.

Another option is the 32 by 32 LED array by Adafruit (product ID: 607). The pitch is 4 mm, and it was used in the original FP implementation<sup>4</sup>. For this option, one can short the resistors at the back of the board (labelled as 'RG1', 'RB3', etc.) and drive the LED in a static mode. With a similar Fourier overlapping percentage in between adjacent acquisitions, the optical flux per unit area is about 1.5-2 times dimmer than that of the first option.

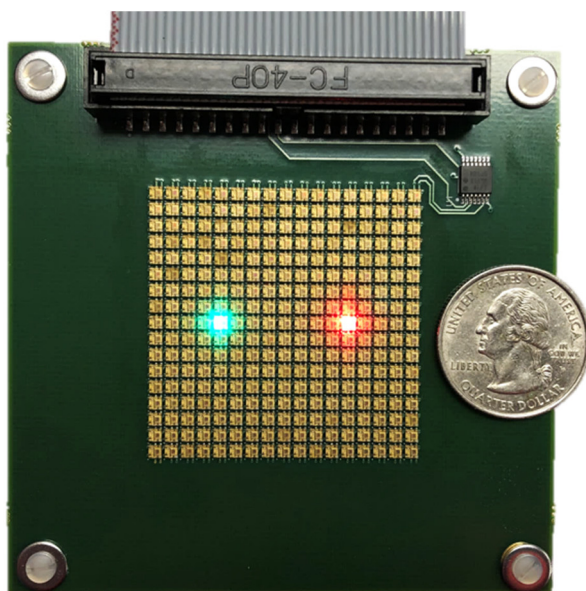


**Figure S1:** A sample programmable LED array built with small and bright SMD LED elements, with a pitch of 2.5 mm. The dense arrangement allows us to bring the array closer to the specimen. It can also be directly placed at the back focal plane of the condenser lens<sup>2,3</sup>.

If the budget allows, one can also build an LED array with high-power LED elements. One option is the Cree XLamp XM-L Color LED, with a pitch of at least 5 mm.

The distance between the specimen and the LED array  $d$  can be set based on the numerical aperture (NA) of the objective lens  $NA_{obj}$  and the pitch of LED array  $p$ . Assuming  $\sim 50\%$  Fourier overlapping percentage at the central region of the Fourier plane, we have  $d = p/(0.5NA_{obj})$ . Considering a 0.1-NA,  $2\times$  objective lens and a 4-mm pitch LED array, the distance between the specimen and the LED array is  $\sim 80$  mm. Similarly, a 2.5 mm pitch LED array gives a distance of  $\sim 50$  mm.

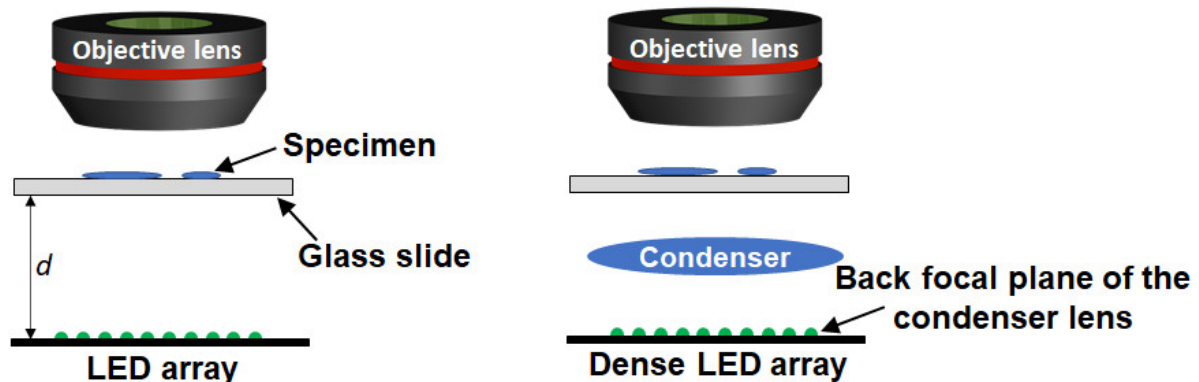


**Figure S2:** For wide-field application using a low-NA objective lens, the LED array can be directly placed underneath the specimen without condenser lens. For higher NA objectives, a dense LED array can be placed at the back focal plane of the condenser for angle-varied illumination, similar to the scheme demonstrated in Ref. <sup>2,3</sup>.

## 2. Objective lens, tube lens, and image sensor

The objective lens and tube lens can be chosen based on an existing upright or inverted microscope platform. For wide-field application, a  $2\times$ , 0.1-NA or  $4\times$ , 0.2-NA objective lens can be used for image acquisition. The LED array can be placed underneath the specimen without condenser lens. For higher NA objectives (easier to satisfy the Fourier aperture overlapping requirement), the LED array can also be placed at the back focal plane of the condenser lens, as shown in Fig. S2.

The options for wide-field objective lenses include, but are not limited to, Nikon  $2\times$  0.1-NA lens, Nikon  $4\times$  0.2-NA lens, Thorlabs TL2X-SAP, and Thorlabs TL4X-SAP. The options for tube lens include, but are not limited to, regular tube lenses from the upright and inverted microscope systems, fixed-focus photographic lenses (e.g., Canon 135 mm, 180 mm, and 200 mm lenses; Nikon 135 mm and 180 mm lenses).

For image sensor, we recommend a cost-effective solution: Sony IMX 183 (20 megapixels, 2.4- $\mu\text{m}$  pixel size, and a quantum efficiency of 79%). The relatively small pixel size of this sensor enables adequate sampling for most configurations. If budget allows, other large-format, high-pixel-count image sensors can also be used for image acquisition; one option is the Sony IMX 540 sensor (24.6 megapixels, 2.74- $\mu\text{m}$  pixel size, and a quantum efficiency of 69%).

### **3. LED intensity calibration and background signal removal**

To calibrate the intensity of different LED elements, we can image an opal diffuser by sequentially turning on each LED element. The average intensity of the captured images can be used to normalize the actual measurements of a sample. Further LED intensity refinement can be performed in the iterative reconstruction process<sup>5</sup>.

Similarly, an empty glass slide can be used to collect the reference darkfield images for background correction. The subtraction of these reference darkfield images (not the average signal) can reduce the impacts of ambient light and stray light in the optical system.

### **4. Image acquisition, data pre-processing, and LED position recovery**

For image acquisition, three different exposure times can be used for different illumination angles. The first exposure time is for brightfield images, where the illumination angles are smaller than the maximum acceptance angle of the objective lens. The second exposure time is used for illumination angles close to the brightfield-darkfield transition region. The third exposure time is for the darkfield images with large illumination angles. For illumination angles in between these three groups, we can acquire the same image with 2 different exposure times for high dynamic range (HDR) combination.

For data pre-processing, we can exclude some regions of the captured image from updating the object solution in the phase retrieval process. Panels **c** and **d** in Box 2 demonstrate two representative cases: the brightfield-to-darkfield transition region and the bright spot caused by the stray light. Binary masks can be generated to locate these regions. When the corresponding images are used as modulus constraints in the updating process, the pixels in the masked white regions will not be used to update the estimated object solution<sup>6</sup>.

For LED position recovery, we can follow the simple procedure discussed in Box 2.

### **5. Iterative phase retrieval process**

In the iterative phase retrieval process, the captured images are often segmented into small tiles (e.g. 256 by 256 pixels) for reconstruction. In this way, the pupil aberration can be treated as spatially invariant across the area of each tile, and the LED illumination can be assumed to be planar across the area of each tile. Figure S3 shows the recovery process using the ptychographic iterative engine<sup>7</sup>. A collection of FP datasets and reconstruction codes are provided for the interested readers<sup>8</sup>. After reconstruction, different tiles can be stitched to form a large field of view image (see, for example, <http://gigapan.com/gigapans/165212> and <http://gigapan.com/gigapans/166861>). Linear alpha blending can be used to remove edge artifacts in-between two adjacent segments<sup>4</sup>.

---

**FP recovery via the ptychographic iterative engine**

---

**Input:** The captured images  $I_n(x, y), n = 1, 2, \dots, N$  (different incident angles); the incident wavevectors from LEDs  $(k_{xn}, k_{yn}), n = 1, 2, \dots, N$ ; the initial pupil aberration  $Pupil(k_x, k_y)$

**Output:** The recovered complex object  $O(x, y)$ ; the updated pupil aberration  $Pupil(k_x, k_y)$

---

**Initialize**  $O(x, y), t = 0$

$\hat{O}(k_x, k_y) = FT\{O(x, y)\}$

**for** loop = 1: iterations

**for**  $n = 1:N$  (different incident angles)

$t = t + 1$  (for adding Nesterov momentum)

$\Psi_n(k_x, k_y) = \hat{O}(k_x - k_{xn}, k_y - k_{yn}) \cdot Pupil(k_x, k_y)$

$\psi_n(x, y) = FT^{-1}\{\Psi_n(k_x, k_y)\}$

$\psi_n^{update}(x, y) = \sqrt{I_n} \cdot \exp\{i \cdot angle[\psi_n(x, y)]\}$  (Fourier magnitude projection)

$\Psi_n^{update}(k_x, k_y) = FT\{\psi_n^{update}(x, y)\}$

$\hat{O}(k_x - k_{xn}, k_y - k_{yn}) = \hat{O}(k_x - k_{xn}, k_y - k_{yn}) + \frac{conj(Pupil(k_x, k_y)) \cdot \{\Psi_n^{update}(k_x, k_y) - \Psi_n(k_x, k_y)\}}{(1 - \alpha_o) |Pupil(k_x, k_y)|^2 + \alpha_o |Pupil(k_x, k_y)|_{max}^2}$

$Pupil(k_x, k_y) = Pupil(k_x, k_y) + \frac{conj(\hat{O}(k_x - k_{xn}, k_y - k_{yn})) \cdot \{\Psi_n^{update}(k_x, k_y) - \Psi_n(k_x, k_y)\}}{(1 - \alpha_p) |\hat{O}(k_x - k_{xn}, k_y - k_{yn})|^2 + \alpha_p |\hat{O}(k_x - k_{xn}, k_y - k_{yn})|_{max}^2}$

**if**  $t == T$

$t = 0$

    add Nesterov momentum

**end**

**end**

**end**

$O(x, y) = FT^{-1}\{\hat{O}(k_x, k_y)\}$

---

**Figure S3:** The flow chart of the FP recovery process using the ptychographic iterative engine<sup>7</sup>.

## References:

- 1 Guo, K., Dong, S., Nanda, P. & Zheng, G. Optimization of sampling pattern and the design of Fourier ptychographic illuminator. *Optics express* **23**, 6171-6180 (2015).
- 2 Guo, K. *et al.* Microscopy illumination engineering using a low-cost liquid crystal display. *Biomedical optics express* **6**, 574-579 (2015).
- 3 Sun, J., Zuo, C., Zhang, L. & Chen, Q. Resolution-enhanced Fourier ptychographic microscopy based on high-numerical-aperture illuminations. *Scientific reports* **7**, 1-11 (2017).
- 4 Zheng, G., Horstmeyer, R. & Yang, C. Wide-field, high-resolution Fourier ptychographic microscopy. *Nature photonics* **7**, 739 (2013).
- 5 Bian, Z., Dong, S. & Zheng, G. Adaptive system correction for robust Fourier ptychographic imaging. *Optics express* **21**, 32400-32410 (2013).
- 6 Dong, S., Bian, Z., Shiradkar, R. & Zheng, G. Sparsely sampled Fourier ptychography. *Optics Express* **22**, 5455-5464, doi:10.1364/OE.22.005455 (2014).
- 7 Maiden, A., Johnson, D. & Li, P. Further improvements to the ptychographical iterative engine. *Optica* **4**, 736-745 (2017).
- 8 Song, P., Jiang, S. & Zheng, G. <https://github.com/SmartImagingLabUConn/Fourier-Ptychography>.